JOURNAL OF PROPULSION AND POWER
Vol. 14, No. 4, July–August 1998

New Model for Intense Self-Similar Vortices

Georgios H. Vatistas*
Concordia University, Montreal, Quebec H3G 1M8, Canada

A new model that is capable of generating single- or double-celled steady, incompressible, intense vortices is proposed. As was evident in earlier experiments, depending on the values of scaling constants, it is shown that the axial-velocity component may attain profiles ranging from jet-like to wake-like. In general, the radial-velocity profile has a similar shape as the tangential velocity, developing a direction reversal near the axis of rotation when the two-celled vortex appears. For the case of a one-celled vortex, the tangential velocity behaves like that of Rankine's vortex with viscous smoothing near the core. However, as the reverse flow inside the core matures the tangential velocity reduces gradually from the forced-vortex profile while its maximum value is augmented. The evolution from a one-celled to a two-celled vortex is also characterized by a migration of the vorticity peak from the central axis toward the core. The present theory suggests that the implementation of the experimental data for the tangential velocity near the core depends on the quality of the secondary flow.

Nomenclature

C = arbitrary constant
f = general function
m, n = constant exponents
P = static pressure, Pa
Re = Reynolds number
r, z = radial and axial cylindrical coordinates
s, t = dummy variables
V = velocity
x, y, z = Cartesian coordinates
α = arbitrary constant
β = scaling constant
Γ = circulation, m^2/s
$\Delta\Pi$ = normalized pressure
δ = normalized pressure
η = scaling constant
η_1, η_2 = model constants
κ = scaling constant
ν = kinematic viscosity, m^2/s
ρ = density, kg/m^3
Ω = vorticity

Subscripts
c = quantity at the vortex core
q = tangential component
r, θ, z = radial, tangential, and axial component
0 = quantity at the vortex center
∞ = dimensional quantity

Superscript
$*$ = dimensional quantity

I. Introduction

THE violent swirling motion of air and water has frightened, fascinated, and frustrated man since antiquity. Today, only a very limited number of technological and naturally occurring flows can be understood without the presence of vortices. Vortices are routinely encountered in many power and propulsion applications. In some applications, such as gas-turbine and vortex combustors, the presence of vortices is essential for the proper operation of the equipment. In others, as in the case of trailing vortices, those generated in the draft tubes of water turbines and those resulting from helicopter blades are an undesirable biproduct of fluid motion, causing a loss of equipment efficiency. These vortices may produce undesirable vibrations and noise making it necessary to discover ways to suppress them. For this reason this phenomenon is considered to be of central importance in fluid dynamics and in related fields.

Fluid vortices can be of different sizes, shapes, and strengths. Their spectrum ranges from the smallest turbulent eddy (10^{-3} m) to planetary vortices (10^{10} m). Depending on their aspect ratio (radius of maximum tangential velocity/height) they may assume a disk- or a columnar-like shape. The region inside the core of $0 \leq$ radius $\leq$ radius of maximum tangential velocity is also known to host a variety of waves. Because of the latter and depending on the prevailing conditions the vortex might develop a "rope"-, "helical"-, or a "sausage"-like core as well as other shapes. Vortices that have most of the axial vorticity component residing within their core are known as *concentrated vortices*. If a tangential velocity is several orders of magnitude larger than the radial and axial components they may be called *intense* or *strong* vortices.

A theoretical description that is capable of capturing the flow details in intense vortices requires the numerical solution of full Navier–Stokes equations. The latter model gives rise to several complexities associated mainly with the unknown boundary conditions and the fact that the tangential velocity dominates the radial and axial-velocity components. Simplified models have been used in the past to study a variety of naturally occurring and industrial problems.

The most elementary of vortex models is by Rankine.[1] This model assumes a linear tangential-velocity distribution inside the core, with a hyperbolic variation outside this core. However, the velocity distribution possesses an unrealistic sharp peak at the point of maximum velocity. In addition, both the radial and axial-velocity components are required to be zero, which presupposes the existence of an external source of energy at the core radius r_c^*, to replenish that dissipated in $1 \leq r < \infty$. Rankine's tangential-velocity profile approximates the actual profile, except near the core. The development of the static pressure distribution is also very reasonable, suggesting that the localized differences of the velocity near r_c^* quietly influence the pressure.

An improved model must take into consideration the smoothing effects of viscosity in the neighborhood of r_c^*. Ro-

Received Aug. 18, 1997; revision received Feb. 4, 1998; accepted for publication Feb. 4, 1998.

*Professor, Mechanical Engineering Department, 1455 DeMaisonneuve Boulevard West. Senior Member AIAA.

senhead[2] proposed an empirical tangential-velocity distribution that has this property. This model simulates the effects of viscosity near the core and assumes no zero radial and axial-velocity components. However, Rosenhead's model underestimates most of the measured values of the tangential velocity near r_c^*.

Burgers'[3] vortex model improves on the correlation between the observed and predicted values for the tangential velocity, but nevertheless assumes a linear profile for the radial velocity and a constant axial velocity.

Vatistas et al.[4] reported on an empirical vortex model that produced a family of bounded velocity distributions. Depending on the value of an exponent, one could obtain tangential-velocity distributions ranging from Rankine's[1] to Rosenhead's.[2] Although all of the velocities were bound in the interval [0, ∞), it produced only a jet-like axial velocity with 100% deficit near the central axis for most of the distributions.

In addition to Rankine's model, where both the radial and axial-velocity components are zero, the models of Refs. 2–4 assumed a one-celled vortex with the general flow pattern in the r–z plane shown qualitatively in Fig. 1a. Sullivan[5] proposed a two-celled vortex characterized by a direction reversal of the radial and axial-velocity components near the axis of rotation. The flow pattern taking place in the r–z plane is shown qualitatively in Fig. 1b. This model produces an unbound radial velocity and a wake-like axial-velocity profile near the center, attaining a constant value asymptotically with the radius.

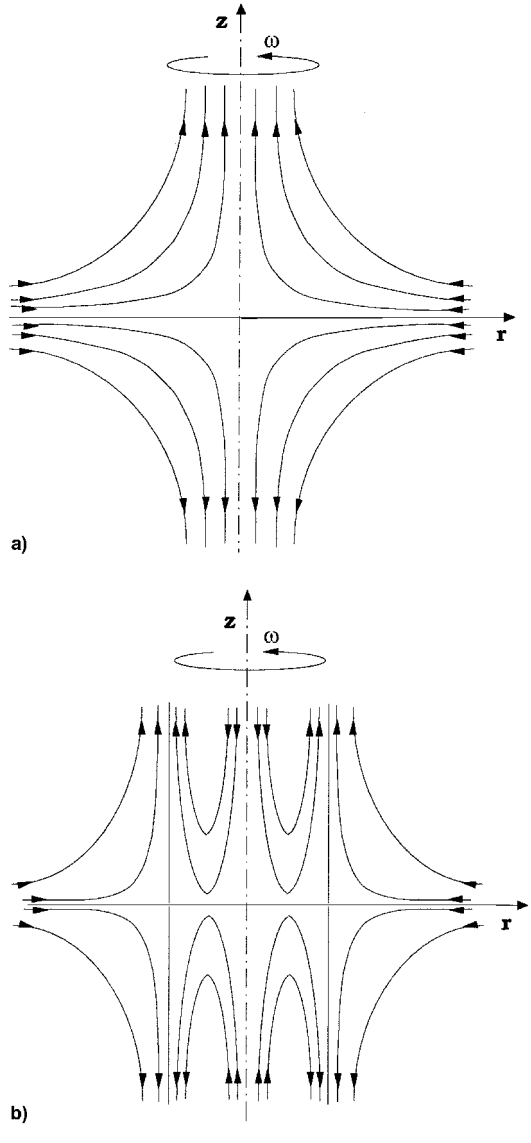

Fig. 1 Schematic of the flow pattern in the r–z plane for a) one- and b) two-celled vortices.

Fernandez-Feria et al.[6] reported on a family of self-similar, nearly inviscid axisymmetric vortices. The tangential velocity that was assumed was proportional to $1/r^{m-2}$. Bultakov et al.[7] presented a numerical solution to a class of self-similar viscous cores assuming a power-law variation for the tangential velocity of the form $V_\theta \approx r^m$.

The present paper reports on a new steady model where, with a proper choice of the scaling parameters, one can produce single- or double-celled intense vortices. It is shown that the axial-velocity component may develop a pure jet-like, or a jet-like with a velocity deficit at the central axis, or a wake-like profile, as in the experiments of Escudier et al.[8] (also see Ref. 9). The radial-velocity profile has, in general, a similar shape as the tangential velocity, in some instances exhibiting a reversal of its direction near the axis of rotation. Both velocity components are several orders of magnitude smaller than the tangential velocity. For the case where a strong reverse flow exists near the central axis, the tangential velocity descends from the well-known forced vortex, and its maximum value increases. The results of previous and present theories are expressed in terms of the nondimensional parameters proposed by Vatistas et al.[10]

II. Formulation of the Problem and Previous Theories

Consider a steady, incompressible columnar vortex. As in most of the vortex models reported previously, the radial and axial-velocity components are assumed to be several orders of magnitude smaller than the tangential velocity, i.e.,

$$V_r = \frac{V_r^*}{V_c^*}, \qquad V_z = \frac{V_z^*}{V_c^*} << 1, \quad \text{or} \quad V_r \text{ and } V_z \approx \mathbb{O}(\delta)$$

and V_θ is only a function of the radius. $V_c^* = \Gamma_z^*/2\pi r_c^*$, and Γ_z^* is the vortex circulation. Under the previous assumptions, the equations of motion in cylindrical coordinates (Fig. 2) are as follows.

Continuity:

$$\frac{\partial V_r}{\partial r} + \frac{V_r}{r} + \frac{\partial V_z}{\partial z} = 0$$

$$\delta \quad \delta \quad \delta$$

r-momentum:

$$V_r\frac{\partial V_r}{\partial r} + V_z\frac{\partial V_r}{\partial z} - \frac{V_\theta^2}{r} = \frac{\partial \Delta P}{\partial r} + \frac{1}{Re}\left(\frac{\partial^2 V_r}{\partial r^2} + \frac{1}{r}\frac{\partial V_r}{\partial r} - \frac{V_r}{r^2} + \frac{\partial^2 V_r}{\partial z^2}\right)$$

$$\delta \ \delta \quad \delta \ \delta \quad 1 \qquad \delta \ \delta \quad \delta \quad \delta \quad \delta$$

z-momentum:

$$V_r\frac{\partial V_z}{\partial r} + V_z\frac{\partial V_z}{\partial z} = \frac{\partial \Delta P}{\partial z} + \frac{1}{Re}\left(\frac{\partial^2 V_z}{\partial r^2} + \frac{1}{r}\frac{\partial V_z}{\partial r} + \frac{\partial^2 V_z}{\partial z^2}\right)$$

$$\delta \ \delta \quad \delta \ \delta \qquad \delta \ \delta \quad \delta \quad \delta$$

θ-*momentum*:

$$V_r\frac{\partial V_\theta}{\partial r} + \frac{V_r V_\theta}{r} = \frac{1}{Re}\left(\frac{\partial^2 V_\theta}{\partial r^2} + \frac{1}{r}\frac{\partial V_\theta}{\partial r} - \frac{V_\theta}{r^2}\right)$$

$$\delta \quad 1 \quad \delta \ 1 \quad \delta \quad 1 \qquad 1 \qquad 1$$

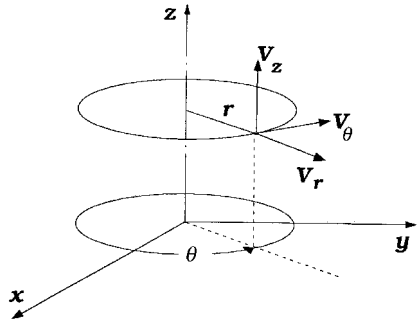

Fig. 2 Coordinate system.

where $r = r^*/r_c^*$, $z = z^*/r_c^*$, $V_\theta = V_\theta^*/V_c^*$, $\Delta P = (P^* - P_\infty^*)/\rho^* V_c^{*2}$, P^* is the pressure, P_∞^* is the pressure far from the vortex center ($r \to \infty$), $Re = V_c^{*2} r_c^*/\nu$, ν^* is the kinematic viscosity, and ρ^* is the density.

Assume further that V_r is a function of the radius, which implies that $V_z = zf n(r)$. In view of the latter assumption and that made previously (that both V_r and V_z are of the order δ), and retaining terms of order δ or higher, the preceding equations simplify as follows.

Continuity:

$$\frac{1}{r}\frac{\mathrm{d}}{\mathrm{d}r}(V_r r) + f(r) = 0 \tag{1}$$

r-momentum:

$$\frac{V_\theta^2}{r} = \frac{\mathrm{d}\Delta P}{\mathrm{d}r} \tag{2}$$

θ-*momentum*:

$$\frac{V_r}{r}\frac{\mathrm{d}}{\mathrm{d}r}(V_\theta r) = \frac{1}{Re}\frac{\mathrm{d}}{\mathrm{d}r}\left[\frac{1}{r}\frac{\mathrm{d}}{\mathrm{d}r}(V_\theta r)\right] \tag{3}$$

while the z-momentum equation indicates that the pressure does not vary along the axial direction.

The vorticity components are given by

$$\Omega_r = -\frac{\partial V_\theta}{\partial z}, \qquad \Omega_z = \frac{\partial V_\theta}{\partial r} + \frac{V_\theta}{r}, \qquad \Omega_\theta = \frac{\partial V_r}{\partial z} - \frac{\partial V_z}{\partial r} \tag{4}$$

$$\delta \qquad\qquad 1 \quad 1 \qquad\qquad \delta \quad \delta$$

where $\Omega_r = (\Omega_r^* r_c^*)/V_c^*$, $\Omega_z = (\Omega_z^* r_c^*))/V_c^*$, and $\Omega_\theta = (\Omega_\theta^* r_c^*)/V_c^*$.

In terms of vorticity, the θ-momentum equation is alternatively given by

$$V_r \Omega_z = \frac{1}{Re}\frac{\mathrm{d}\Omega_z}{\mathrm{d}r}$$

Based on the preceding equation it is worthwhile to note that the diffusion of vorticity is balanced by an equal convection carried by the radial-velocity component.

The pressure is obtained from the r-momentum equation

$$\Delta\Pi = \frac{\displaystyle\int_0^r \frac{V_\theta^2}{r}\,\mathrm{d}r}{\displaystyle\int_0^\infty \frac{V_\theta^2}{r}\,\mathrm{d}r} \tag{5}$$

where $\Delta\Pi = (P^* - P_\infty^*)/(P_0^* - P_\infty^*)$.

Considering the order of magnitude of the individual terms, the vorticity components can be simplified into

$$\Omega_z = \frac{1}{r}\frac{\mathrm{d}}{\mathrm{d}r}(V_\theta r), \qquad \Omega_r = \Omega_\theta \approx 0 \tag{6}$$

Utilization of the preceding outlined postulates produced several simple models in the past that were discussed in the Introduction of this paper. The velocity, vorticity, and radial pressure distributions of past theories are depicted in Fig. 3. Formulas for the velocity components associated with these models are summarized in Table 1, and the degrees of vortex concentration are given in Table 2. It can be seen from Table 2 that the limits of concentrated vortices are the Rankine's vortex,[1] where all of the vorticity resides inside the core, and Rosenhead's model,[2] where half of the vorticity is concentrated in the core. In all of the previously mentioned theories the steady vortex is maintained by transporting vorticity from large radii toward the center by the radial velocity to replenish that already dissipated. In Sullivan's case,[5] however, not only is vorticity transported from afar by the radial-velocity toward the core, it is also driven away from the center. As a result the vorticity develops peaks near but not at the center of rotation. The value of $\eta_2 = 6.238$ in Sullivan's model (Table 1) is the root of the following equation

$$2\eta_2 \exp\left(-\eta_2 + 3\int_0^{\eta_2}\frac{1 - e^{-s}}{s}\,\mathrm{d}s\right) - \int_0^{\eta_2}\exp\left(-t + 3\int_0^t \frac{1 - e^{-s}}{s}\,\mathrm{d}s\right)\mathrm{d}t = 0$$

which ensures that the maximum tangential velocity takes place at $r = 1$. The value of η_2 has been found numerically.

III. New Vortex Model

The starting point of the present model is with the work of Escudier et al.,[8] who demonstrated experimentally that the axial-velocity component is able to develop profiles ranging from jet-like to wake-like shapes. In an attempt to qualitatively simulate this behavior, we assume an axial-velocity variation of the form

$$\frac{V_z}{z} = 2\alpha\left[\frac{1}{(1 + \eta\beta r^2)^2} - \frac{\kappa}{(1 + \beta r^2)^2}\right] \tag{7}$$

where α, κ, η, and β are constants. From continuity, Eq. (1), the radial velocity is

$$V_r = \alpha r\left(\frac{\kappa}{1 + \beta r^2} - \frac{1}{1 + \eta\beta r^2}\right) \tag{8}$$

Integration of Eq. (3) yields

$$\frac{1}{r}\frac{\mathrm{d}}{\mathrm{d}r}(V_\theta r) = C_\infty \frac{(1 + \beta r^2)^{(\alpha\kappa Re/2\beta)}}{(1 + \eta\beta r^2)^{(\alpha Re/2\beta\eta)}}$$

or

$$\frac{1}{r}\frac{\mathrm{d}}{\mathrm{d}r}(V_\theta r) = C_\infty\left[\frac{1 + \beta r^2}{(1 + \eta\beta r^2)^{(1/\eta\kappa)}}\right]^m$$

where C_∞ is a constant, and $m = \alpha\kappa Re/2\beta$. A second integration of Eq. (3) produces the following expression for the tangential velocity:

$$V_\theta = \frac{C_\infty}{r}\int_0^r\left[\frac{1 + \beta r^2}{(1 + \eta\beta r^2)^{(1/\eta\kappa)}}\right]^m r\,\mathrm{d}r \tag{9}$$

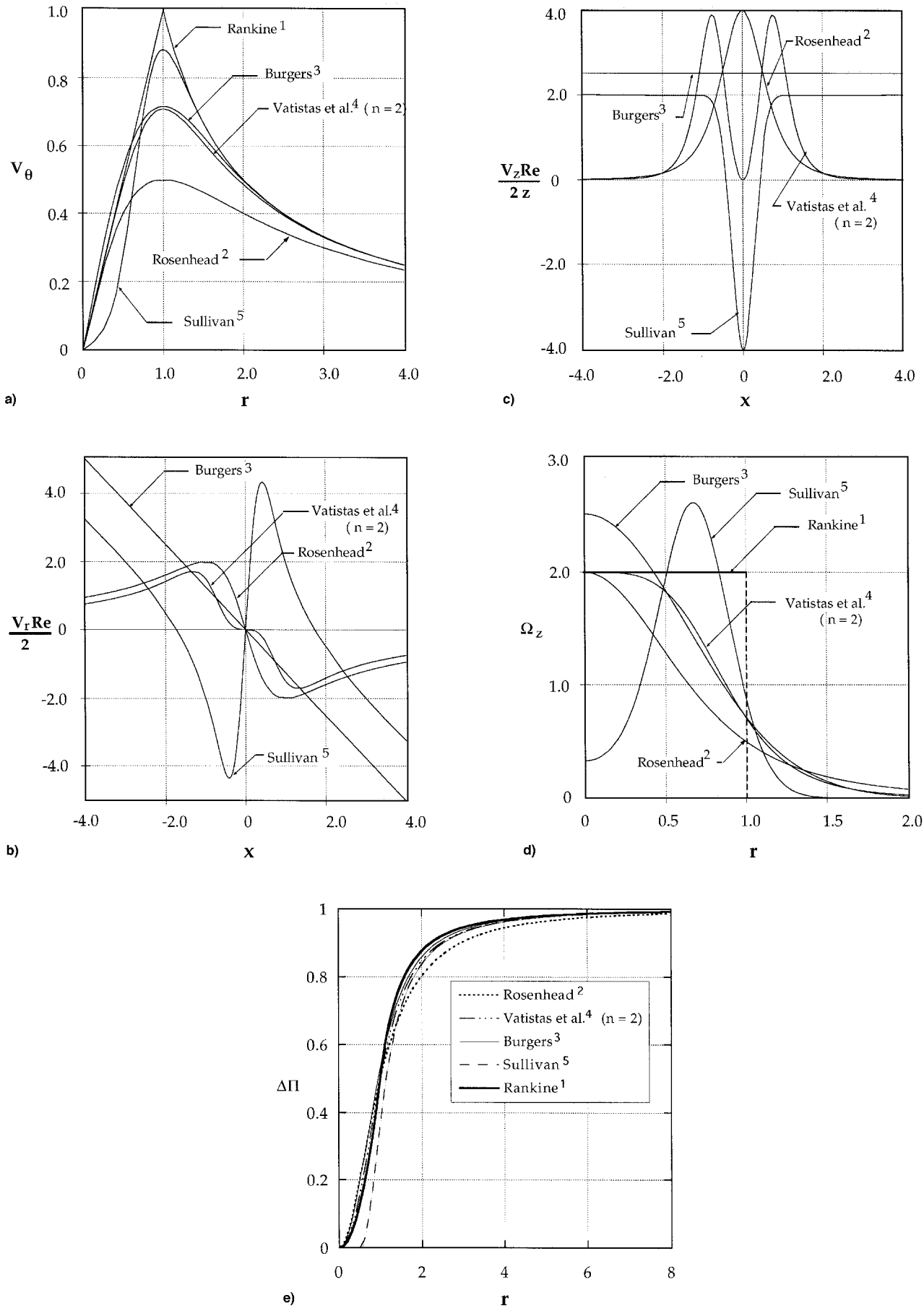

Fig. 3 Profiles of the a) tangential-velocity, b) radial-velocity, c) axial-velocity, d) vorticity, and e) static pressure from previous theories.

Table 1 Velocity formulas for past vortex models

Vortex model	V_θ	V_r	V_z/z
Rankine[1]	r, for r in [0, 1] $1/r$, for r in [0, ∞)	0	0
Rosenhead[2]	$\dfrac{r}{1+r^2}$	$-\dfrac{4}{Re}\dfrac{r}{1+r^2}$	$\dfrac{8}{Re}\dfrac{1}{(1+r^2)^2}$
Burgers[3]	$\dfrac{1}{r}[1-\exp(-\eta_1 r^2)]$	$-\dfrac{2\eta_1}{Re}r$	$\dfrac{4\eta_1}{Re}$
Vatistas et al.[4]	$\dfrac{r}{(1+r^{2n_1})^{1/n_1}}$	$-\dfrac{2(n_1+1)}{Re}\dfrac{r^{2n_1-1}}{1+r^{2n_1}}$	$\dfrac{4n_1(n_1+1)}{Re}\dfrac{r^2(n_1-1)}{(1+r^{2n_1})^2}$
Sullivan[5]	$\dfrac{1}{r}\dfrac{H(\eta_2 r^2)}{\lim_{r\to\infty}H(\eta_2 r^2)}$	$\dfrac{2}{Re}\left\{-r+\dfrac{3}{r}[1-\exp(-\eta_2 r^2)]\right\}$	$\dfrac{4}{Re}[1-3\exp(-\eta_2 r^2)]$

Note: $\eta_1 = 1.256$, $\eta_2 = 6.238$, and $H(\eta_2 r^2) = \int_0^{\eta_2 r^2}\exp[-t + 3\int_0^t (1-e^{-s})/s\,ds]\,dt$.

Table 2 Percentage of vorticity inside the core for past vortex models

Vortex model	Percentage of vorticity
Rankine[1]	100.00
Rosenhead[2]	50.00
Burgers[3]	71.05
Vatistas et al.[4] (for $n = 2$)	70.70
Sullivan[5]	88.30

Table 3 Percentage of vorticity inside the core for the present model

κ	Percentage of vorticity
0.00	63.01
0.40	64.96
0.50	65.70
0.60	66.71
0.70	68.02
0.80	69.85
0.90	72.67
1.00	77.76
1.03	80.32
1.08	87.22
1.10	91.42

Note: $\eta = 0.625$, $\beta = 0.600$.

The constant C_∞ is evaluated using the boundary condition $V_\theta r \to 1$, when $r \to \infty$. Therefore

$$C_\infty = 1 \Big/ \int_0^\infty \left[\frac{1+\beta r^2}{(1+\eta\beta r^2)^{(1/\eta\kappa)}}\right]^m r\,dr$$

Given the values of the scaling constants η, β, and κ, m must be chosen in such a way as to allow the tangential velocity to attain its maximum value at $r = 1$. This requirement is obtained realizing that $(dV_\theta/dr)_{r=1} = 0$, or

$$m\log\left[\frac{1+\beta}{(1+\eta\beta)^{\eta\kappa}}\right] - \log\int_0^1\left[\frac{1+\beta r^2}{(1+\eta\beta r^2)^{(1/\eta\kappa)}}\right]^m r\,dr = 0 \tag{10}$$

The values for integral and the root are found numerically.

In terms of the constants η, β, and κ, noting that $\alpha = 2\eta\beta/Re\kappa$, the radial- and axial-velocity components are given respectively, by,

$$\frac{V_r Re\kappa}{2m\beta} = r\left(\frac{\kappa}{1+\beta r^2} - \frac{1}{1+\eta\beta r^2}\right) \tag{11}$$

$$\frac{V_z Re\kappa}{2zm\beta} = 2\left[\frac{1}{(1+\eta\beta r^2)^2} - \frac{\kappa}{(1+\beta r^2)^2}\right] \tag{12}$$

The vorticity is given by

$$\Omega_z = C_\infty\left[\frac{1+\beta r^2}{(1+\eta\beta r^2)^{(1/\eta\kappa)}}\right]^m \tag{13}$$

whereas the pressure distribution is obtained numerically with Eq. (5), using the expression of the tangential velocity given by Eq. (9).

Tangential-velocity profiles for different values of κ, with $\eta = 0.625$ and $\beta = 0.600$, together with past experimental data[4,11–18] are given in Fig. 4. When the values of κ are small, the familiar Rankine-like profile with a velocity smoothing effect near the core is apparent. The value of the maximum velocity increases with κ. For values of $\kappa > 1.00$ the maximum velocity value increases, and the tangential-velocity reduces gradually from the forced-vortex profile. Consistent with the assumption that the static pressure develops in such a manner as to balance the centrifugal force, it produces the profiles shown in Fig. 5. It is evident from Fig. 5 that there is a very small difference in the pressure variation for the given κ. Because the differences of the static pressure are well within the experimental error, one cannot in a reliable manner recover the tangential velocity from the experimental pressure data.[10,13,15,20]

However, one cannot make conclusions with respect to the flow behavior taking the tangential velocity and pressure in isolation. It is very important to investigate the behavior of the other two velocity components. For small values of κ (Fig. 6), the radial velocity is negative and increases in value as the radius becomes smaller, transporting the required vorticity from a large distance away. The axial velocity exhibits a jet-like behavior similar to a Gaussian distribution (Fig. 7). As the value of κ increases the maximum radial velocity increases, while the axial becomes smaller and its distribution grows *fatter*. At $\kappa = 0.70$ the axial velocity has developed a depression at the center that increases with κ. For $\kappa = 1.00$ a saddle-like profile at $r = 0$ for the radial velocity is noticeable. At this condition the axial-velocity profile exhibits a 100% deficit at the vortex center. A further increment of κ produces a two-celled vortex that is characterized by a secondary flow taking place inside the core that gives rise into a wake-like, axial-velocity profile. Because the vorticity is simultaneously transported from a large distance, and away from the center, the vorticity develops the peaks near the core, as shown in Fig. 8.

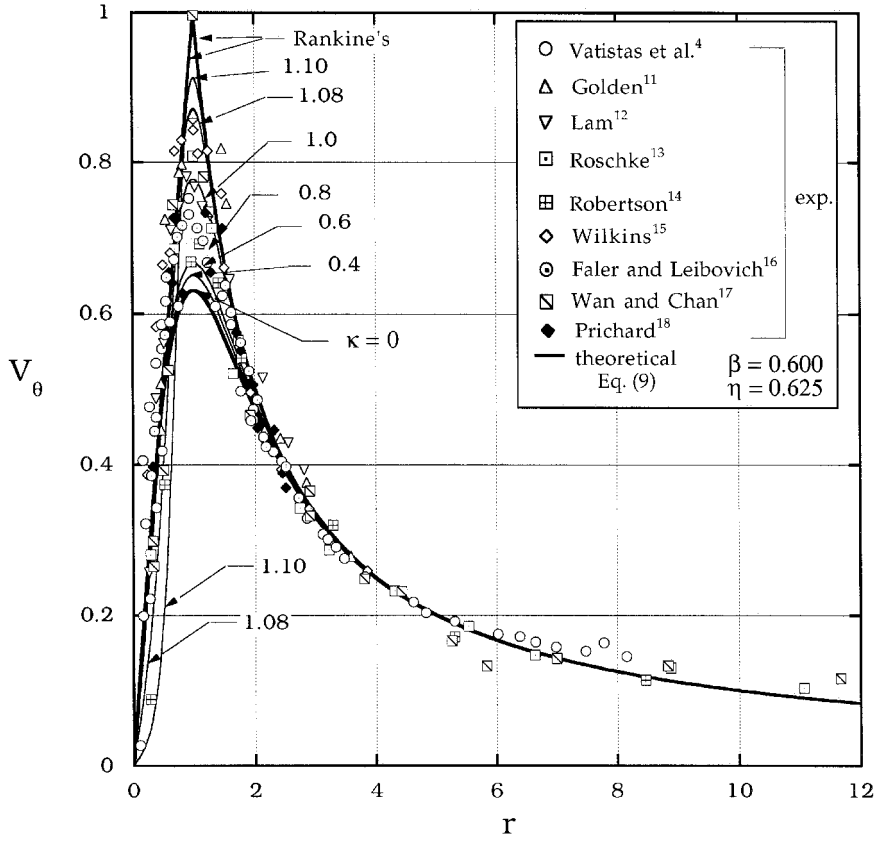

Fig. 4 Comparisons of the tangential velocity from the present theory and previous experimental data.

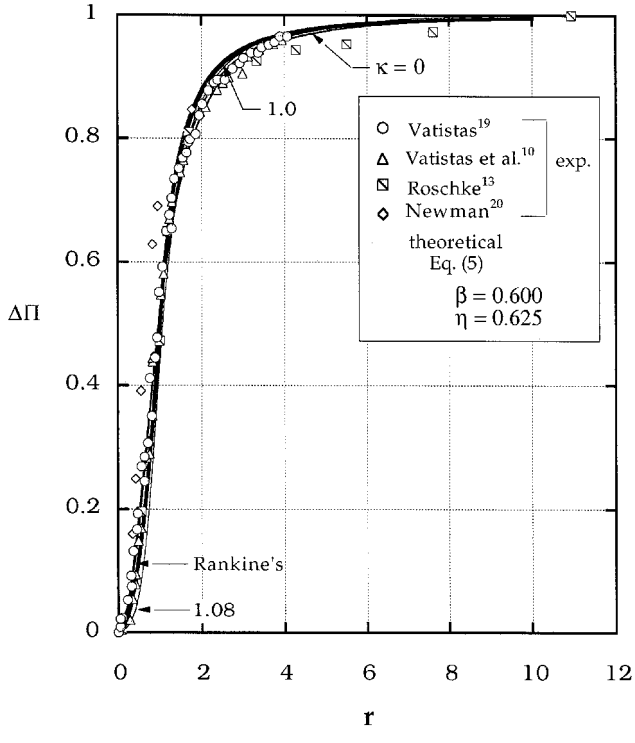

Fig. 5 Comparisons of the static pressure from the present theory and previous experimental data.

The percentage of vorticity inside the core for the present model, as a function of κ, is given in Table 3.

Considering the complexity of the problem, previously made comparisons of the experimental tangential-velocity profiles with different theories that produce a single distribution for the velocity were generally fair, with the exception being the neighborhood of the core where the maximum spread of the experimental points were noted. According to the present results this area happens to be the sector where the secondary flow influences the tangential-velocity distribution. Therefore, it is hardly plausible to be able to represent the velocity and pressure by single universal profiles having the forms $V_\theta = f_n(r)$ and $\Delta\Pi = f_n(r)$, respectively. The distinct features of the secondary flow near the core must also be taken into consideration. Although specific values for the scaling constants (η and β) were used in the presentation of results outlined earlier, other choices of values will produce different magnitudes for the flow properties, but the main distinct features of the flow will be preserved.

For the case where κ = 0 the flow properties, the velocity components and vorticity are, respectively,

$$\frac{V_r Re}{2m\varepsilon} = -\frac{r}{1 + \varepsilon r^2} \tag{14}$$

$$\frac{V_z Re}{2zm\varepsilon} = \frac{2}{(1 + \varepsilon r^2)^2} \tag{15}$$

$$V_\theta = \frac{(1 + \varepsilon r^2)^{m-1} - 1}{r(1 + \varepsilon r^2)^{m-1}} \tag{16}$$

$$\Omega_z = \frac{2(m - 1)\varepsilon}{(1 + \varepsilon r^2)^m} \tag{17}$$

where $\varepsilon = \eta\beta$. The exponent m can be calculated using the maximum tangential condition $(dV_\theta/dr)_{r=1} = 0$, which yields

$$2\varepsilon(1 + \varepsilon)^{m-1} - 2\varepsilon(m - 1)[(1 + \varepsilon)^{m-1} - 1] - (1 + \varepsilon)[(1 + \varepsilon)^{m-1} - 1] = 0 \tag{18}$$

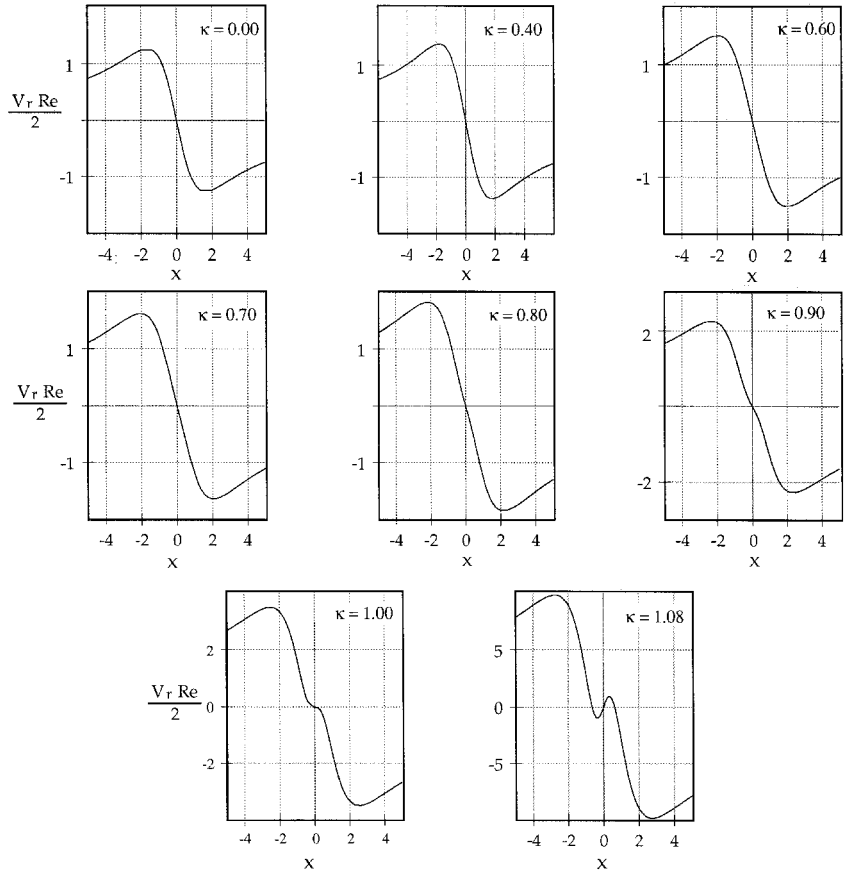

Fig. 6 Radial-velocity profiles, present theory.

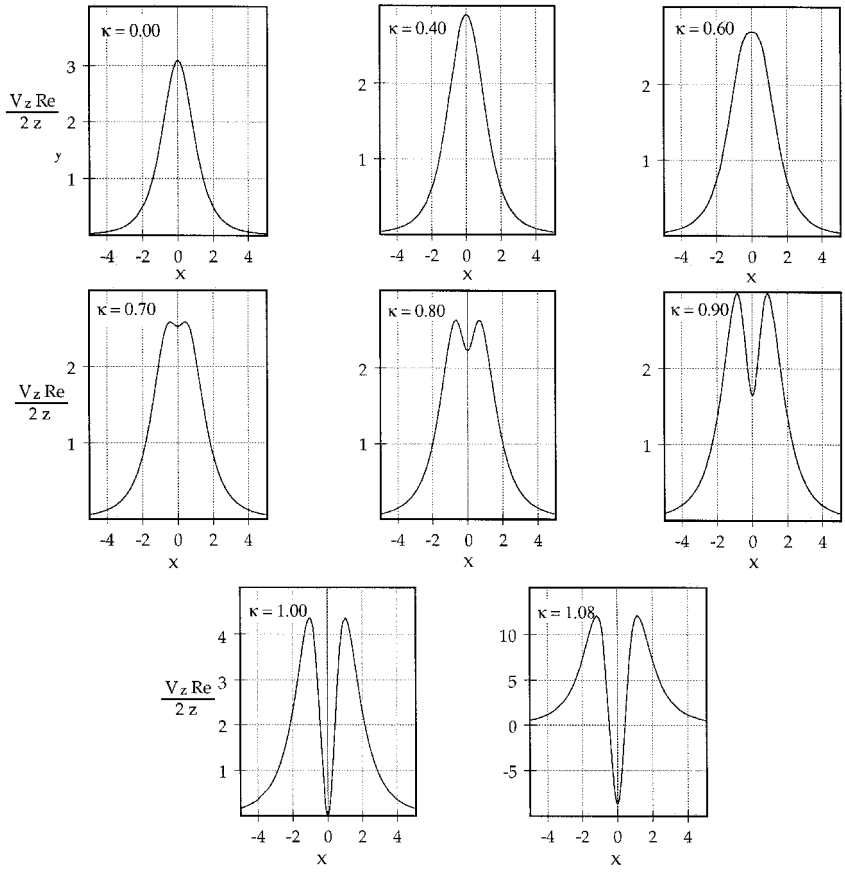

Fig. 7 Axial-velocity profiles, present theory.

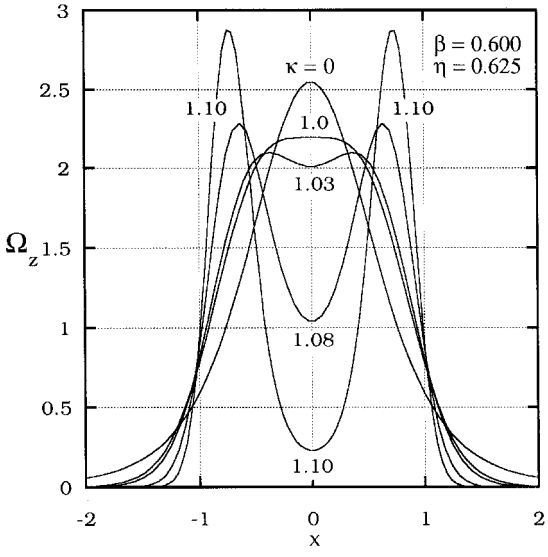

Fig. 8 Vorticity profiles, present theory.

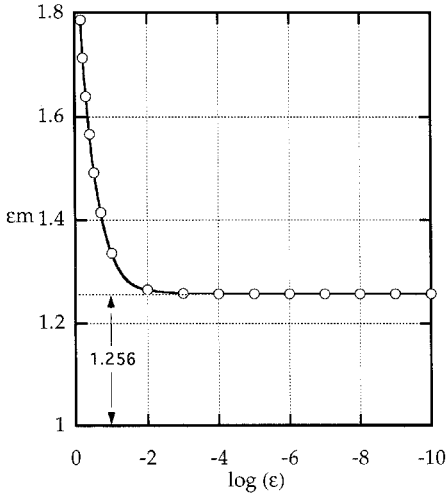

Fig. 9 Relationship between parameters εm vs ε for single-cell vortices.

For $\varepsilon = 1$, Rosenhead's[2] vortex is obtained. It can be seen from Fig. 9 that as $\varepsilon \to 0$, $m\varepsilon \to 1.256$ or the vortex tends to Burgers' model.[3] For values of ε in (0, 1] one can produce values for the flow properties that lie between these two vortex models.

IV. Conclusions

A model for single- or double-celled intense vortices was presented. Depending on the values of scaling constants, it was shown that the axial-velocity component may attain profiles ranging from jet-like to wake-like, which are consistent with previous experimental information. As the reverse flow inside the core developed, the tangential velocity reduced gradually from the forced-vortex profile and the magnitude of the maximum velocity increased. The transition from a one-celled to a two-celled vortex was characterized by the departure of the vorticity peak from the central axis to a region near the core. The present analysis suggested that it may not be possible to represent the velocity and pressure distributions by single universal profiles of the radius. The effects of the secondary flow near the core must also be included. The latter inclusion gives rise to a family of self-similar profiles for the fluid parameters involved. Because of the relative insensitivity of the pressure on the tangential velocity, it is also concluded that this velocity cannot be recovered reliably from the experimental pressure data. All flow properties in the present model are bounded over the entire semi-infinite domain.

References

[1]Rankine, W. J. M., *Manual of Applied Mechanics*, C. Griffen Co., London, 1858.

[2]Rosenhead, L., "The Spread of Vorticity in the Wake Behind a Cylinder," *Proceedings of the Royal Society of London, Series A: Mathematical and Physical Sciences*, Vol. 127, 1930, pp. 73–76.

[3]Burgers, J. M., "A Mathematical Model Illustrating the Theory of Turbulence," *Advances in Applied Mechanics*, Vol. 1, 1948, pp. 171–199.

[4]Vatistas, G. H., Kozel, V., and Mih, C. W., "A Simpler Model for Concentrated Vortices," *Experiments in Fluids*, Vol. 11, 1991, pp. 73–76.

[5]Sullivan, R. D., "A Two-Cell Vortex Solution of the Navier-Stokes Equations," *Journal of the Aerospace Sciences*, Vol. 26, No. 11, 1959, pp. 767, 768.

[6]Fernandez-Feria, R., Fernandez dela Mora, J., and Barrero, A. "Solution Breakdown in a Family of Self-Similar Nearly Inviscid Axisymmetric Vortices," *Journal of Fluid Mechanics*, Vol. 105, 1995, pp. 77–91.

[7]Buldakov, E., Sychev, V., and Yegorov, I. "Viscous Core of Tornado-Like Flow," AIAA Paper 97-1786, June 1997.

[8]Escudier, M. P., Bornstein, J., and Zehnder, N. "Observations and LDA Measurements of Confined Turbulent Vortex Flow," *Journal of Fluid Mechanics*, Vol. 98, Pt. 1, 1980, pp. 49–63.

[9]Escudier, M. P., Bornstein, J., and Maxworthy T., "The Dynamics of Confined Vortices," *Proceedings of the Royal Society of London, Series A: Mathematical and Physical Sciences*, Vol. 382, 1982, pp. 335–360.

[10]Vatistas, G. H., Lin, S., and Li, P. M. "A Similar Profile for the Tangential Velocity in Vortex Chambers," *Experiments in Fluids*, Vol. 6, 1988, pp. 135–137.

[11]Golden, J. H., "The Life of Florida Key's Waterspouts. I," *Journal of Applied Meteorology*, Vol. 13, 1974, pp. 676–688.

[12]Lam, H. C., "An Experimental Investigation and Dimensional Analysis of Confined Vortex Flows," Ph.D Dissertation, Dept. of Mechanical Engineering, Concordia Univ., Montreal, PQ, Canada, 1993.

[13]Roschke, E. J., "Experimental Investigation of a Confined, Jet-Driven Water Vortex," Jet Propulsion Lab., Rept. 32-982, NASA CR-78550, Oct. 1966.

[14]Robertson, J. M., *Hydrodynamics in Theory and Application*, Prentice–Hall, Engelwood Cliffs, NJ, 1966.

[15]Wilkins, F. M., "The Role of Electrical Phenomena Associated Tornadoes," *Journal of Geophysical Research*, Vol. 69, No. 12, 1964, pp. 2435–2447.

[16]Faler, J. H., and Leibovich, S., "Disturbed States of Vortex Flow and Vortex Breakdown," *Physics of Fluids*, Vol. 20, 1977, pp. 1385–1400.

[17]Wan, C. A., and Chan, C. C., "Measurement of the Velocity Field in a Simulated Tornado-Like Vortex Using a Three-Dimensional Velocity Probe," *Journal of Atmospheric Sciences*, Vol. 29, 1971, pp. 116–127.

[18]Prichard, W. G., "Solitary Waves in Rotating Fluids," *Journal of Fluid Mechanics*, Vol. 42, Pt. 1, 1970, pp. 61–83.

[19]Vatistas, G. H., "Analysis of Fine Particle Concentrations in a Confined Vortex," *Journal of Hydraulic Research*, Vol. 27, No. 3, 1989, pp. 417–427.

[20]Newman, B. G., "Flow in a Viscous Trailing Vortex," *Aeronautical Quarterly*, Vol. 10, 1959, pp. 149–162.